
Differences in gas venting from ultramafic-hosted warm springs: the example of Oman and Voltri Ophiolites

Boulart Cedric^{1, 2, *}, Chavagnac Valerie¹, Monnin Christophe¹, Delacour Adeline^{1, 3}, Ceuleneer Georges¹, Hoareau Guilhem⁴

¹ Geosciences Environnement Toulouse, UMR5563 CNRS/UPS/IRD/CNES, 14 Avenue Edouard Belin, 31400 Toulouse, France

² IFREMER, Géosciences Marines, Laboratoire Géochimie-Métallogénie, BP 70, 29280 Plouzané, France

³ Université Jean Monnet, UMR CNRS 6524, Laboratoire Magmas et Volcans, 23 rue du Docteur Paul Michelon, 42023 Saint Etienne Cedex 2, France

⁴ Université de Pau et des Pays de l'Adour, UMR CNRS TOTAL 5150, IPRA Avenue de l'Université, 64013 Pau Cedex, France

*: Corresponding author : Cédric Boulart, email address : cedric.boulart@ifremer.fr

Abstract:

Serpentinisation of mantle rocks, leading to natural venting of hydrogen and methane, has been reported to occur at the global scale, wherever fluids percolate in ultramafic formations. Here we compare gas composition from two on-land, low-temperature, and hyper-alkaline springs hosted on ultramafic rocks in the ophiolite massifs of the Sultanate of Oman and the Ligurian Alps (Voltri Group, Genoa region, Northern Italy). These two settings exhibit similar chemical and mineralogical features but show diverse styles of gas venting. Commonly to all hyper-alkaline springs, gases are characterised by relatively high N₂, very low O₂ and CO₂ concentrations, and a strong enrichment in H₂ and CH₄. The comparison between Oman and Liguria highlights a high variability of the H₂/CH₄ ratios whereby the gas phase of the Oman Ophiolite is enriched in H₂ whereas being CH₄ enriched in the Voltri Ophiolite. These results combined with literature data define three groups that may reflect different stages of serpentinisation producing fluids from hydrogen-dominated to methane-dominated. The origin of these distinct groups might lie in the difference of the mineralogical composition of the rocks within which the fluids circulate, on the degree of alteration of the rocks and finally on the geological/metamorphic history of the ophiolite.

Keywords: Methane ; hydrogen ; gas composition ; hyper-alkaline springs ; Oman ; Voltri Massif

1. Introduction

Natural venting of hydrogen (H₂) and associated methane (CH₄) is a common feature of fluid rock interaction, and in particular of serpentinisation of ultramafic rocks. In the last ten years, this phenomenon has gained significant interest in the scientific and industrial communities, from prebiotic chemistry and astrobiology to energy and mineral resource exploration. Serpentinisation reactions – i.e. the alteration of mantle peridotites by fluids of various origin (e.g. meteoric, seawater) – may naturally produce high amounts of H₂, which leads subsequently to the abiotic formation of CH₄ and possibly higher hydrocarbon (HC) chains via Fischer-Tropsch-Type (FTT) reactions. This FTT process occurs when faults allow fluid penetration within the peridotites and have been identified in different settings: along fracture zones, passive margins, at the wall of rift valleys, at mid-ocean ridges (e.g., Cannat et al., 2010; Charlou et al., 2010), and also in deep igneous and metasedimentary rocks (Sherwood Lollar et al., 2006).

51 It is now clear that wherever ultramafic rocks are percolated by fluids, alkaline springs
52 are present. In the Deep Sea, a few hydrothermal vents lying on ultramafic rocks are known
53 today, including either high-temperature vent fields (>350°C) such as Rainbow, Logatchev
54 and Ashadze (Charlou et al., 2002; Fouquet et al., 2008; Lein et al., 2000), or low-temperature
55 ones (~100°C) such as Lost City vent field (Kelley et al., 2005; Proskurowski et al., 2008). In
56 recent years, several ones were identified and/or suspected on ultra-slow spreading ridges, e.g.
57 Knipovich, Gakkel and Cayman ridges (Bach et al., 2002; Connelly et al., 2012). On-land,
58 percolation of meteoric water in obducted ophiolite massif produces low-temperature hyper-
59 alkaline springs, which are considered as “analogues” of the Lost City vent field off the Mid-
60 Atlantic Ridge. They are reported in Oman (Chavagnac et al., 2013a, 2013b; Neal and Stanger,
61 1983; Sano et al., 1993), Philippines (Abrajano et al., 1988), Turkey (Etiope et al., 2011;
62 Hosgormez, 2007), Italy (Chavagnac et al., 2013a, 2013b; Cipolli et al., 2004, Schwarzenbach
63 et al., 2013), California (Blank et al., 2009), Cyprus (Neal and Shand, 2002), Greece (Etiope
64 et al., 2013a), Portugal (Etiope et al., 2013b; Marques et al., 2008), British Columbia (Power
65 et al., 2007), New Zealand (Lyon et al., 1990) and New Caledonia (Boulart et al., 2012;
66 Launay and Fontes, 1985), amongst others. The main differences between submarine vents
67 and on-land warm springs are the nature of the percolating water, i.e. seawater and meteoric
68 fluids, respectively, as well as venting temperature, which is lower than 100°C in the
69 continental settings. This reveals that the development of hydrogen and methane venting in
70 ultramafic-hosted environment may encompass a broad range of conditions (pressure,
71 temperature, water/rock ratio, etc...) leading to various degrees of advancement in the
72 chemical reactions for the production of natural H₂ and CH₄.

73 Serpentine results from the interaction of water with Fe-Mg rich minerals, i.e. olivine
74 and pyroxene. During the serpentinisation reactions, Fe²⁺ contained in olivine is oxidised to
75 Fe³⁺ (which may lead to the formation of secondary magnetite) while water reduction

76 produces hydrogen and aqueous hydroxyl responsible for high pH values. Hydrocarbon gases
77 may be generated abiotically via FTT reactions (i.e. Sabatier reaction) through the reduction
78 of carbon dioxide by H₂ to form CH₄ and longer-chain HC (Holm and Charlou, 2001;
79 Ingmanson and Dowler, 1977; Konn et al., 2009a, 2009b; Shock, 1990). Serpentinisation is
80 thus accompanied by the production of methane and light alkanes (Ague, 2000). Note that
81 low-temperature hyper-alkaline waters have lost all their dissolved inorganic carbon (DIC)
82 during the course of serpentinisation reactions (Chavagnac et al., 2013a; Sader et al., 2007).

83 Large quantities of CH₄ and lesser amounts of light alkanes can be produced by FTT
84 reactions when they are catalysed by magnetite, chromite or awaruite at temperatures around
85 300°C (Berndt et al., 1996; McCollom and Seewald, 2001, 2007), but also at lower
86 temperatures (de Boer et al., 2007; Etiope et al., 2013a; Hosgormez, 2007, Neubeck et al.,
87 2011). Nevertheless, the sole abiotic origin of HC in ultramafic environments remains
88 questionable in the sense that biologically produced methane can be present at the same
89 locations and it is difficult to distinguish between the two processes (Bradley and Summons,
90 2010; Etiope et al., 2011; Konn et al., 2009a, 2009b; Sherwood Lollar et al., 2006).

91 In this contribution, we report new data on the gas chemical composition from two on-
92 land, low-temperature, and hyper-alkaline warm springs hosted on ultramafic rocks of the
93 ophiolite massifs of the Sultanate of Oman and the Ligurian Alps (Voltri group, Genoa region,
94 Northern Italy). The present dataset complements the ones of Neal and Stanger (1983) and
95 Sano et al. (1993), who first reported the composition of the gases venting in the hyper-
96 alkaline springs of Oman. The composition of gases bubbling in the Ligurian springs is given
97 by Boschetti et al. (2013), Cipolli et al. (2004) and Schwarzenbach (2011). Alteration of these
98 two ophiolites by meteoric waters generates hyper-alkaline springs with a pH > 9 and similar
99 chemical and mineralogical features (Chavagnac et al., 2013a, 2013b) but with great
100 differences in their gas chemical composition.

101

102 **2. Geological Settings**

103

104 ***2.1. Oman Ophiolite***

105 The Semail Nappe in the Northern Mountain of the Sultanate of Oman (Figure 1) is one of the
106 largest (~ 30.000 Km²) and best exposed (thanks to semi-arid climate) fragment of the oceanic
107 Tethys lithosphere on land (Glennie et al., 1973). Its geological evolution includes magmatic
108 accretion along an oceanic spreading centre in a short time laps from ~97 to ~95 Ma
109 (Goodenough et al., 2010; Rioux et al., 2013; Tilton et al., 1981; Tippit et al., 1981)
110 immediately followed by intra-oceanic thrusting in a near-ridge environment (Boudier et al.,
111 1985; Lanphere, 1981; Montigny et al., 1988). Its obduction onto the Arabian margin
112 occurred about 70 m.y. ago (Glennie et al., 1973). Petrological and geochemical signatures of
113 igneous rocks of this ophiolite are clearly MORB-related in several districts (Benoit et al.,
114 1996; Ceuleneer et al., 1996; Python and Ceuleneer, 2003; Python et al., 2008). Elsewhere
115 parent melts have a more ambiguous signature that can be attributed to nascent subduction
116 (Pearce et al., 1981) or to incorporation of very-high temperature hydrothermal water in a
117 spreading setting (inducing hydrated melting and modifying liquid lines of descent). A thick
118 pile of neritic carbonates deposited on the top of the ophiolite after subsidence of the Oman
119 margin (Glennie et al., 1973). The present exposure of the ophiolite is related to recent (Mio-
120 Pliocene) uplift of the Oman mountains, likely a prelude to the future collision with Eurasia
121 (Fournier et al., 2006). Alkaline springs are essentially located in two particular settings: i) at
122 the basal contact between autochthonous sediments and mantle peridotites, and ii) at the
123 contact between the mantle peridotites and the cumulates from the crustal section (the
124 paleo“Moho”). Rare springs are located within the mantle or within the crustal section, away
125 from these major geological discontinuities. When present, these springs and gas vents are

126 located along faults and shear discontinuity zones in the serpentinised ultramafic section, but
127 also in less altered peridotites and gabbroic sections. Release of gases can be directly seen
128 from bubbling within the wadi bed (local Arabic name for small rivers). Gas discharge is also
129 evidenced by pockmarks forming in the precipitates accumulating in the riverbed (Chavagnac
130 et al., 2013a). Neal and Stanger (1983) estimated the gas flows from 10 mL/sec up to 10 L/sec
131 at Nizwa and B'lad (station 29) for the highest flows (Figure 1).

132 Although the present climate in Oman is quite dry (117 mm/year average annual
133 rainfall; Kwarteng et al., 2009), the region was characterised rather recently (a period centred
134 on 8.200 years BP) by a much more humid climate with intense rain events related to the end
135 of the last glacial period (Burns et al., 2001). It is likely that a large proportion of the
136 underground aquifers of Oman were refilled during this period, enabling the perennial flow of
137 hyper-alkaline waters (Clark and Fontes, 1990; Dewandel et al., 2005).

138

139 ***2.2. Voltri Group, Liguria, Italy***

140 In Liguria, the studied area is located in the Voltri Massif, which is part of the Penninic
141 ophiolites (Internal Ligurides) and forms the transition between the Alps and the Appenine
142 (Figure 2). It is the largest ophiolite massif in the Alps-Appenine system (Brouwer et al., 2002)
143 composed of three main units: i) a calcschist unit consisting of blueschist to eclogite-facies
144 calcareous metasediments, metavolcanics and slices of serpentinites (Voltri-Rossiglione Unit),
145 ii) a serpentinite unit with highly-altered peridotites including eclogitic metagabbros and
146 metabasalts (Beigua Unit) and, iii) a lherzolite unit (Erro-Tobbio Unit) (Brouwer et al., 2002;
147 Bruni et al., 2002; Capponi et al., 1994; Cipolli et al., 2004; Vignaroli et al., 2010).

148 The Voltri group is derived from the Western Tethys ocean that separated European
149 and Adriatic plates in the Middle Jurassic (Bill et al., 2001). It is considered as on-land
150 analogues of oceanic lithosphere originated at slow-spreading ridges (Barrett and Spooner,

151 1977). Indeed, the chemistry of the Beigua metagabbros indicates a tholeiitic origin typical of
152 mid-ocean ridges magmatism (Brouwer et al., 2002). The Piedmont-Ligurian Ocean was later
153 (Early Cretaceous) subject to subduction and collision leading to the emplacement of oceanic
154 units onto the European continental crust (Brouwer et al., 2002).

155 Most of the hyper-alkaline springs found by Cipolli et al. (2004) are located within the
156 Beigua Unit composed of metagabbros and metabasalts that underwent multistage
157 metamorphic evolution in blueschist to eclogite facies. Only a couple of these springs are
158 hosted on altered lherzolites of the Erro-Tobbio Unit (Figure 2). These springs emerge along
159 faults and fractures through serpentinites and related rocks.

160 Springs are usually located in the riverbeds, just above the water level and often
161 harnessed with tubing. Direct gas bubbling was observed only at 3 locations (GOR34, GOR35,
162 L43; Figure 2) but the discharge was very irregular, sometimes absent for several minutes.

163

164 **3. Sampling and analyses**

165

166 Sampling was performed in June 2010 in Liguria and in January 2011 in Oman. Sampling
167 sites were chosen from a database kindly provided by the Ministry of Water Resources of
168 Oman, while in Liguria, sampling sites were chosen from the database published in Cipolli et
169 al. (2004). Details on locations, hosting lithology/mineralogy, as well as basic chemical
170 composition of the spring waters (pH, temperature, major cations and anions) are summarised
171 in Table 1 and is extensively discussed in Chavagnac et al. (2013b).

172 21 gas samples from 9 sites were collected in Oman directly from the springs (Figure
173 1). In Liguria, a total of 12 samples were collected from the 3 sites where active bubbling was
174 observed (L43, GOR34, GOR35, Figure 2). All gas samples were collected into crimp-sealed
175 gas glass bottles by water displacement. Dissolved gas samples were also collected at all sites

176 visited in 2010 (7 sites, 15 samples in Liguria) and 2011 (12 sites, 23 samples in Oman) into
177 poisoned (HgCl_2), crimp-sealed glass bottles. Dissolved gases were then analysed using the
178 headspace method (Kolb and Ettre, 1997) followed by gas chromatography in the same way
179 as the gas samples, using a SRI 8610C gas chromatograph, fitted with a Flame Ionization
180 Detector/Methanizer (FID-M) for the detection of methane (CH_4), small alkanes ($\text{C}_1\text{-C}_5$), CO
181 and CO_2 , and a Helium Ionization Detector (HID) for the detection of hydrogen (H_2), oxygen
182 (O_2), and nitrogen (N_2). Methane gas is eluted together with CO and CO_2 on a 3' Molecular
183 Sieve Packed Column, using Hydrogen as the carrier gas, while H_2 , O_2 , and N_2 are eluted on 6'
184 Silica Gel Packed Column with Helium as the carrier gas.

185 In both cases, gas compositions are given as non-dried gases, taken into account the
186 water vapour phase.

187

188 **4. Results and discussion**

189

190 ***4.1. Water chemistry and gas compositions***

191 The full chemical composition of the hyper-alkaline fluids collected in Oman and Liguria and
192 the composition of the associated mineralogical assemblages formed therein are presented in
193 Chavagnac et al. (2013a, 2013b). For clarity we here summarise the composition, temperature
194 and pH, together with the precipitate mineralogy and geological context (Table 1).
195 Composition of the gas phase and the concentration of dissolved gases in the alkaline waters
196 are given, respectively, in Tables 2 and 3. All the springs investigated in this study discharge
197 hyper-alkaline waters, whose pH values range from 9.5 to 11.7 in Liguria, and from 10.1 to
198 11.9 in Oman. These waters all belong to the Ca-OH hydro-chemical group characterised by
199 very low magnesium and DIC contents (Table 1) (Chavagnac et al., 2013b). The Ca-OH type
200 – also described as mature waters as they evolved from rainwater to neutral Mg-HCO_3 waters

201 and to high-pH Ca-OH type waters (Bruni et al., 2002) – is typical of waters circulating in a
202 deep and closed ultramafic rocks system affected by present-day, low-temperature
203 serpentinisation (Bruni et al., 2002; Chavagnac et al., 2013b; Etiope et al., 2013a; Neal and
204 Shand, 2002, Schwarzenbach et al., 2013). According to these results, the gases, analysed in
205 this study, are venting from waters coming from a deep aquifer, mainly hosted by
206 serpentinised peridotites and related rocks (Bruni et al., 2002).

207 Temperatures vary from 21.4 to 23.7°C in Ligurian springs while they range from 20.9
208 to 29.9°C in Oman. These temperatures are very similar (although slightly higher in Oman
209 springs) while the local climatic conditions are obviously very different between Oman and
210 Northern Italy. Chavagnac et al. (2013b) noted that there was no significant influence of the
211 seasonal variation on the spring water temperature both in Oman and Liguria. As indicated by
212 Neal and Stanger (1984), these temperatures indicate that the water cannot penetrate deeper
213 than the base of the ultramafic formation in Oman, i.e. 5 km.

214 All the gas samples at both locations are strongly enriched in N₂ and have very low O₂
215 partial pressures (Tables 2 and 3). This leads to a gas phase N₂/O₂ ratio varying from 130 to
216 440 in Oman and 417 to 848 in Liguria (atmospheric ratio is ~1.9). These values are similar to
217 those found by Etiope et al. (2013a) in the Othrys ophiolite springs (Archani, Greece) as well
218 as other world-wide hyper-alkaline springs (Abrajano et al., 1988; Cipolli et al., 2004; Neal
219 and Stanger, 1983). Dissolved N₂ and O₂ concentrations vary between 656 to 2135 µM and 5.7
220 to 23.4 µM, respectively in Oman, and from 600 to 3785 µM and from 3.2 to 31.6 µM,
221 respectively in Liguria. Waters are therefore supersaturated in N₂ (the equilibrium
222 concentration at T=25°C and Salinity = 0.5 is ~400 µM; Hamme and Emerson, 2004) while
223 the dissolved O₂ concentration is below the concentration of a water body at equilibrium with
224 the atmosphere (402 µM at T=25°C and Salinity = 0.5; Green, 1958). The low O_{2(aq)} content,
225 also observed by Etiope et al. (2013a) in Greece and Boschetti et al. (2013) in Italy, is a

226 characteristic of hyper-alkaline waters and is due to the reducing conditions linked to
227 hydrogen production during serpentinisation process. The actual presence of O₂ in our
228 samples may be due to (air?) contamination during sampling. Similar explanation could be
229 suggested for the high N₂ concentrations; however, contamination alone cannot account the
230 high N₂ content of the gas phase. As reported by Etiope et al. (2013a), variability in dissolved
231 N₂ and O₂ concentrations may rather be related to the meteoric water input into the upwelling
232 spring water, especially in Liguria whereby average annual rainfall is ten times higher than in
233 Oman.

234 Malatesta et al. (2011) argue that the Voltri Massif exhumed within a serpentinite
235 “channel” whereby plutonic and sedimentary rocks metamorphosed at different pressure and
236 temperature conditions are mixed during their pathway to the surface, wrapped by chlorite–
237 amphibole–talc schists (e.g. Hoogerduijn Strating, 1991). Within these metamorphic rocks,
238 the low-strain serpentinised peridotites contain higher nitrogen concentration (4-6 ppm) than
239 their high-pressure counterparts (1-3 ppm), but still much lower than metasedimentary rocks
240 (100-1700 ppm) (Busigny et al., 2003; Philippot et al., 2007). In the latter, N₂ occurs as
241 ammonium (NH₄) and is substituting potassium in K-bearing minerals (Busigny et al., 2003).
242 The higher N₂/O₂ and K/Cl ratios of Liguria samples compared to the Oman ones (as shown
243 in Figure 3) suggest that serpentinisation-derived waters were in contact with the
244 metasedimentary formation along their pathway, leaching N₂ from the rocks. Note that the
245 nitrogen in the metasedimentary formation was not released during subduction (Philippot et
246 al., 2007).

247 Another typical feature of low-temperature hyper-alkaline springs is the low
248 concentration in CO₂, both in the gas phase (this work) and in the waters (Chavagnac et al.,
249 2013b). Our measurements (Tables 2 and 3) are therefore coherent with most of the findings
250 in other ophiolites in the world (Abrajano et al., 1988; Etiope et al., 2011, 2013a; Neal and

251 Stanger, 1983). In Oman, CO₂ was detected neither in the gas phase nor in the aqueous phase,
252 while in Liguria, CO₂ is significantly present at concentrations up to 22 μM in the aqueous
253 phase and up to 130 ppm in the vapour phase (actual atmospheric CO₂ ~350 ppm). The
254 extremely low concentration in CO₂ (below detection limit) in high-pH waters of Oman
255 shows that there is no supply of atmospheric CO₂ to these waters (as suggested by Pfeifer,
256 1977).

257 Oman and Voltri hyper-alkaline springs are characterised by a very low DIC content
258 (Chavagnac et al., 2013b, Schwarzenbach et al., 2013; and therefore a very low equilibrium
259 pCO₂) enabling the absorption of atmospheric CO₂ by the waters. This is evidenced by the
260 formation of a thin layer of carbonate precipitates (calcite and/or aragonite) in Oman springs
261 (Table 1, Chavagnac et al., 2013a). At the same time, there may be consumption of CO₂ in
262 waters to form CH₄ and other HC during the FTT reactions (see §4.2).

263

264 ***4.2.H₂ and hydrocarbons (C1-C5)***

265 Enrichment of the gas phase in H₂ and CH₄ (Tables 2 and 3) is typical of hyper-alkaline
266 springs. However, a striking difference between Oman and Liguria is in the amount of H_{2(g)}
267 compared to CH_{4(g)}. Comparison between Oman and Liguria shows indeed very different
268 styles of H₂ and CH₄ venting while the main geological setting (ultramafic rocks) and the
269 environmental conditions (T, pH) appear similar.

270 A comparison of H₂/CH₄ ratios for other ultrabasic formations, as depicted in Figure 4,
271 points to three groups: i) a H₂-dominated group including Oman, Rainbow, Lost City,
272 Logatchev and Socorro Island (Neal and Stanger, 1983; Charlou et al., 2002; Proskurowski et
273 al., 2008; Schmidt et al., 2008; Taran et al., 2010); ii) a CH₄-dominated including the
274 Tekirova Ophiolite (Turkey) (Etiope et al., 2011), the Othrys Ophiolite (Greece) (Etiope et al.,
275 2013a) together with our samples from the Ligurian Alps; iii) a third group, which includes

276 the Zambales ophiolite (Abrajano et al., 1988) and the Bay of Prony (New Caledonia)
277 (Boulart et al., 2012), is intermediate with a ratio close to 1-2. Interestingly, the H₂-
278 dominated group is mostly constituted by vents developing along mid-ocean ridges and
279 characterised by higher temperatures, although Lost City is a low-temperature system
280 compared to Rainbow or Logatchev (Charlou et al., 2002; Proskurowski et al., 2008).
281 Nevertheless, fluid temperatures of the seafloor vents are significantly higher than those of
282 on-land hyperalkaline springs, which are overall below 40°C. The Oman ophiolite is the sole
283 belonging to the H₂-dominated group. This may be related to a simpler geological history than
284 the other ophiolites, as it was not included in the Alpine collision belt contrary to the CH₄-
285 dominated ophiolites. Indeed, the latter have undergone multi-stage metamorphism during the
286 collision event and their obduction onto the continent.

287 We propose that the data depicted in Figure 4 may be related to the influence of
288 geodynamic and geologic context on serpentinisation reactions. The first argument comes
289 from the locations of the hyper-alkaline springs from which gas bubbling is clearly observed.
290 Indeed, in Oman, gas samples were collected from hyper-alkaline springs emerging from the
291 major structural discontinuity at the transition between crustal section and mantle rock (paleo-
292 Moho), and none from hyper-alkaline springs located nearby the basal thrust plane, e.g. the
293 metamorphic structural discontinuity (Chavagnac et al., 2013b). In contrast, gas bubbling in
294 Liguria was observed only at three hyper-alkaline springs emerging from various
295 metamorphosed substratum (highly serpentinised metabasalt/metagabbros and serpentinised
296 lherzolites) wrapped by chlorite–amphibole–talc schists (Hoogerduijn Strating, 1991). These
297 schists may have been used as a conduit by meteoric waters to infiltrate and interact with the
298 substratum, explaining the high N₂ gas content of Liguria hyper-alkaline springs.

299

300 - *Hydrogen*

301 In Oman, H₂ is the second dominant gas after N₂ in the gas phase, ranging from 9.4% (site 27)
302 to 12.1% (site 28) of the total gas volume. The lowest dissolved H₂ concentrations were found
303 in the wadi at site 20 (26.7 to 65 µmol/l) while the highest values were found at site 28 (377
304 µmol/l). This agrees with the concentrations previously measured (Neal and Stanger, 1983;
305 Sano et al., 1993). Note that H₂ concentrations given by Neal and Stanger (1983) – up to 99%
306 vol – are much higher than ours, probably as a consequence of the different methodologies
307 used for gas measurements and of the fact that Neal and Stanger (1983) values might not have
308 taken into account the water vapour in the total gas volume.

309 In the Voltri Group, H_{2(g)} concentrations range from 0.011% (L43) to 1.2% (GOR34)
310 of the total gas volume, i.e. 10 to 100 times lower than in Oman. Dissolved H₂ concentrations
311 are relatively low (up to to 5 µmol/l on average) except for two sites (C11 and LER2) where
312 the concentrations are higher (up to 562.6 µmol/l at LER2). A strong variability between
313 samples from the same site can be observed although conditions of sampling were identical
314 from one sample to the other, which may depict a sporadic venting of H₂. This remains to be
315 confirmed by further measurements.

316 The low H₂ content in the Voltri samples, also reported by Boschetti et al. (2013) for
317 the Voltri Group as well as by Etiope et al. (2013a) in another setting in Greece, seems to be
318 uncommon for hyper-alkaline environments. During the reactions of serpentinisation at
319 moderate temperatures (<300°C), olivine and pyroxene react with water to form serpentine,
320 brucite, magnetite and various Fe/Ni alloys depending on redox conditions of reactions. Other
321 phases such as talc, amphibole (e.g. tremolite), chlorite and sulfides can complete the
322 parageneses. In fact, as noted by Mevel (2003), this is a succession of simple reactions
323 starting with the silicate dissolution leading to the production of SiO_{2(aq)}, which then reacts
324 with Mg²⁺ and OH⁻ to form the serpentine crystal and the secondary minerals. In the same
325 time, water reacts with metals in silicates, i.e. oxidizing Fe²⁺ contained in olivine into Fe³⁺

326 which can be incorporated both in serpentine and magnetite (O'Hanley and Dyar, 1993;
327 Evans, 2008; Andreani et al., 2013), and reducing H₂O to H_{2(g)}. Hence, the assemblage
328 serpentine-brucite determines the silica activity of the system, which subsequently controls
329 the oxidation of Fe²⁺ to Fe³⁺ and therefore H_{2(g)} production (Evans, 2008; Katayama et al.,
330 2010). Seyfried et al. (2007) also showed in laboratory experiments that a high silica activity
331 could limit the production of H₂. Low H₂ content is then supported by SiO₂ concentrations
332 measured in the Ligurian fluids, which are significantly higher than in Oman (Table 1,
333 Chavagnac et al., 2013b). Our data in Oman and Liguria may therefore suggest a first low-
334 silica activity stage producing high amounts of H₂ (Oman) followed by a second stage of
335 higher silica activity derived from the altered mafic rocks, limiting the production of H₂
336 (Liguria). Episode of a low silica activity fluid metasomatism (rodingitization) is a common
337 feature of ophiolite complexes, taking place primarily during ocean-floor metamorphism and
338 evidenced in terms of lithologies by the occurrence of epidote-rich to diopside-rich rocks in or
339 adjacent to serpentinites (e.g. Schandl et al., 1989). Diopsidites and rodingites were identified
340 both in Oman (Python et al., 2007) and in Liguria (e.g. Dal Piaz et al., 1980). Ferrando et al.
341 (2010) suggest that ophiolite complexes (i.e. the Alpine orogeny), which are subducted then
342 exhumed, may undergo additional episode(s) of serpentinitisation and rodingitization during
343 the prograde to retrograde metamorphic path. This would be evidenced by the occurrence of
344 H₂-rich fluid inclusions (and also a Ca metasomatism), but these are rarely preserved and
345 detected in metamorphic environments. However, Peretti et al. (1992) report the occurrence of
346 fluid inclusions in the Malenco peridotites composed of H₂ (0.3–3 mol.% of the total gas)
347 within brines (5.1 wt.% CaCl₂ + 6.4 wt.% NaCl) and Ferrando et al. (2010) described fluid
348 inclusions in Bellecombe meta-ophiolites made up 1.0 and 0.4 mol% of H₂ and CH₄,
349 respectively, within brines (6 wt.% CaCl₂ + 6 wt.% NaCl). While both studies illustrate a
350 second episode of Ca-rich and Si-undersaturated reducing fluid percolation, it is unclear

351 whether this event is related to the prograde or late stage metamorphic history of the Alpine
352 orogeny. Nevertheless, these authors clearly identified that H₂-rich serpentinisation-related
353 fluid was produced before the final exhumation of the ophiolite complex.

354 In addition, temperature and water-rock ratio are two other parameters that have a
355 strong control on Fe speciation during serpentinisation and therefore on H₂ production, as
356 discussed by Klein et al. (2009). In their model calculations, they indicate that at low
357 temperatures (<150-200°C) and low water-rock ratios (<0.1 to 5), hydrogen production is
358 related to the formation of Fe³⁺-serpentine. Andreani et al. (2013) reported similar results on
359 the role of Fe³⁺-serpentine on H₂ production based on a μ -XANES study of Fe-speciation in
360 serpentine minerals. Besides, they stated that Fe³⁺ goes predominantly into serpentine, rather
361 than into magnetite, for serpentinisation degree up to 75%.

362 As emphasised in Hellevang et al. (2011), the presence of nitrogen, sulfur and carbon
363 compounds in various redox states may also affect the H₂ generation by limiting the degree of
364 reduction of the aqueous solutions. As for instance, Hellevang et al. (2011) simulated the
365 effect of carbon species on the potential for H₂ generation from an aqueous solution of olivine
366 (Fo90). In natural aquatic systems, the dissolved CO₂ reacts with H₂O to form H₂CO₃, HCO₃⁻
367 and CO₃²⁻. However, due to the serpentinisation reactions, conditions are increasingly
368 reducing, which thermodynamically favour reduction of inorganic carbon to CH₄. Hellevang
369 et al. (2011) summarised the equilibrium as the following:



371 According to their experiments, at low carbon content, the aqueous solution is rapidly reduced
372 and allows the formation of significant amounts of H₂. On the opposite, at higher carbon
373 content, more olivine is required to form significant H₂ quantities. In the same experiments, at
374 constant C content, the CO₂ partial pressure decreases as CO₂ is converted to CH₄, allowing
375 O₂ activity to drop, which favours H₂ formation. In our case, the presence of CO₂ both in the

376 gas and aqueous phase from Liguria indicates that the CO₂ is not completely converted to
377 CH₄; hence the aqueous solution may not be significantly reduced to allow H₂ formation at
378 significant levels.

379 In Oman, the absence of CO₂ in both gas and aqueous phases indicates that all the CO₂
380 is either converted to CH₄ or consumed by carbonate formation. This is confirmed by the
381 relationship between O₂ and H₂ (Figure 5; Hellevang et al., 2011), which shows that H₂
382 generation might be also controlled by the introduction of O₂ in the system.

383

384 - *Methane and hydrocarbons*

385 In Oman, CH_{4(g)}, the third most abundant gas, ranges from 1.5% at sites 11 and 13 up to 8% at
386 site 31. In the dissolved phase, concentrations in CH₄ vary from 7.4 µmol/l at site 26 to 209.2
387 µmol/l at site 30. In Liguria, CH₄ is the second dominant gas after N₂, sometimes the first.
388 The lowest contents were observed at GOR35 (10.5% of the total gas volume) and the highest
389 at L43 (37%). L43 was also characterised by the highest dissolved CH₄ concentration (649.4
390 µmol/l, the water-atmosphere equilibrium concentration for this station is 2.3 nmol/l), while
391 the lowest was measured at LER2. Intermediate concentrations (~300 µmol/l) were found at
392 C11 and BR1.

393 It is commonly accepted that CH₄ and possibly longer hydrocarbons are forming in
394 hyper-alkaline fluids abiogenically, through the FTT reactions as the following (Abrajano et
395 al., 1988; Charlou et al., 2002; Hosgormez, 2007; Proskurowski et al., 2008):



397 Carbon isotopic composition data previously collected in Oman and Liguria undoubtedly
398 indicate the abiogenic origin of CH₄ (δ¹³C₁ ~ -9‰; Boschetti et al., 2013; Neal and Stanger,
399 1983). However, one cannot exclude another synthesis pathway, which consists in the
400 reduction of formic acid, formaldehyde, methanol and later CH₄ (Seewald et al., 2006).

401 FTT reactions have been studied for more than a century, to synthesize CH₄ and
402 alkanes from CO at high temperature. However, the efficiency of FTT synthesis from CO₂ (i.e.
403 methanation) is lower under aqueous hydrothermal conditions (Foustoukos and Seyfried,
404 2004). Provided the presence of catalysts (i.e. magnetite, awaruite and chromite) and at high
405 temperature (>300°C), FTT reactions from CO₂ can nevertheless produce high amounts of
406 CH₄ and light alkanes (Berndt et al., 1996; Horita and Berndt, 1999; McCollom and Seewald,
407 2001). More recently, Neubeck et al. (2011) studied the generation of H₂ and CH₄, in the 30-
408 70°C range, and demonstrated that the presence of H₂, CO, CO₂ and the necessary catalysts
409 (i.e. magnetite, chromite among others) leads to the generation of CH₄ in a few months, even
410 at low temperature. In fact, in the absence of catalysts, methanation is thermodynamically
411 favoured at temperatures below 100°C although it evolves slowly over time (Etiope et al.,
412 2013a). The relationship between dissolved SiO₂ and CH₄ in Liguria (Figure 6) shows that the
413 production of CH₄ is controlled by dissolved SiO₂ and therefore by the dissolution of olivine.
414 This is in line with Neubeck et al. (2011) who showed that the dissolved CH₄ concentration is
415 a proxy for olivine dissolution rates.

416 Besides the role of the catalysts, Oze and Sharma (2005) proposed a possible
417 formation of CH₄ without H₂ mediation during serpentinisation in abundant CO₂ conditions,
418 which is the case in Ligurian springs. However, it is difficult today to establish the role of
419 each parameter, especially since H₂ may be consumed as it is produced, maintaining its
420 concentration at a low level. We may suggest that the high concentration in CH₄ in both the
421 gas and the aqueous phase in Liguria is the result of the FTT reactions, occurring at a later
422 stage of the serpentinisation process while in Oman, the lower amount of magnetite as well as
423 the low content in CH₄ tend to support that the serpentinisation process is at an earlier stage.
424 Nevertheless, we cannot exclude the fact that the availability of carbon in Oman might be a
425 limiting factor for FTT reactions, which is not the case in Liguria (Schwarzenbach et al.,

426 2013).

427 Traces of light alkanes were found in the gas phase both in Liguria and in Oman.
428 Samples from Liguria showed concentrations of C₂ ranging from 20 ppmV (GOR35) to 441
429 ppmV (L43), but no HC with longer chains were detected. In Oman, C₂ was present in all
430 samples, from 8.2 ppmV in the wadi (site 20) to 108.9 ppmV at site 27. Higher alkanes (up to
431 C₄) were found only at site 11 with variable concentrations. Only at sites 11 and 30, dissolved
432 C₂ was detected (up to 240 nmol/l) in the spring waters. No dissolved alkanes (C₂ to C₄) were
433 detected in the dissolved phase in the Ligurian samples.

434 Although finding light alkanes as in our Oman and Ligurian samples is common for
435 ultramafic fluids, their origin remains subject to debate (Proskurowski et al., 2008; Konn et al.,
436 2009a). In the Tekirova ophiolite (Turkey), Etiope et al. (2011) and Hosgormez (2007)
437 showed from the isotopic compositions that the alkanes were not all produced by FTT-
438 reactions, but more probably originated from a strong thermogenic component. However,
439 isotopic studies cannot prove the abiogenic origin of longer-chained HC (>C₅) since a variety
440 of mostly unknown fractionation steps may occur along the synthesis pathways, with a
441 dominance of biogenic source and/or processes hiding their characteristic signature (Konn et
442 al., 2009a).

443 Although the carbon isotope composition is not yet available for our gas samples, a
444 first estimate of the light alkane distribution can be made with the Schulz-Flory method
445 (Figure 7; Flory, 1936). Indeed, the product distribution of hydrocarbons formed during the
446 FTT-reactions generally follows the Schulz-Flory distribution, which is expressed as the
447 following equation:

$$448 \frac{W}{n} = (1 - \alpha)^{n-1} \alpha^{n-1} \quad (3)$$

449 where W is the molar fraction of HC molecules, n the number of C atoms and α the chain
450 growth probability factor. As a result, the distribution of HC is controlled by the chain growth

451 probability factor, which is typical of abiotic synthesis.

452 Our data in Oman do not fit this model, confirming that part of the light alkanes are
453 probably generated through degradation of organic matter or thermogenesis in the same way
454 as in Tekirova ophiolite (Etiope et al., 2011). This is especially true for higher hydrocarbons
455 (above C₃). We may suggest that this is also the case of the Voltri ophiolite although longer-
456 chain HC were not detected with our methodology. However, the amount of C₂ seems to be
457 associated with the amount of CH₄, taking into account that the gas venting from the
458 metaperidotites of the Erro-Tobbio coincides with those of the Oman crustal section/peridotite,
459 which are undistinguishable from one another (Figure 8). Adding the data from Boschetti et al.
460 (2013) to Figure 8 confirms this trend with an R² above 0.85. This tends to indicate that C₂ is
461 derived from abiogenic polymerisation, which has been experimentally demonstrated earlier
462 in Des Marais et al. (1981) by 'spark-discharge' gas phase experiments. However, as noted by
463 Proskurowski (2010), uncatalysed polymerisation remains to be proven in aqueous conditions.
464

465 5. Concluding remarks

466 Serpentinisation is a phenomenon that occurs wherever mantle rocks are altered by aqueous
467 fluids. The alteration of the Oman and Liguria ophiolites by meteoric waters indeed generates
468 hyper-alkaline fluids with pH up to 11-12 at temperatures of 20-40°C at the springs. This is
469 accompanied by the production of a gas phase enriched in hydrogen and subsequently
470 methane. Comparison of the gas composition from Oman and Liguria, and more generally
471 from various places over the world, shows significant differences in terms of H₂/CH₄ ratios.
472 Three groups have been identified likely related to different stages in the serpentinisation
473 reactions, from the hydrogen-dominated to the methane-dominated fluids. The distinction
474 between these groups might lie in the difference of rock mineralogical composition in which
475 the fluids circulate, on the degree of rock alteration and finally on the geological history of the

476 ophiolite. To fully understand the present-day serpentinisation reactions leading to the
477 formation of hydrogen, it is necessary to know the depth and the nature (rock composition) of
478 the reaction zone, which remains an undocumented black box to-date.

479 The comparison of the Oman and Liguria cases with other hyper-alkaline springs
480 worldwide illustrates even more the diversity of gas venting within ultramafic environments
481 and the complexity of the chemical reactions, which may be controlled by the geodynamic
482 and the geological context. It is clear that ophiolites have evolved differently since their
483 obduction, especially in the context of the Alpine collision belt. The resulting metamorphic
484 history has therefore an impact on the gas composition of the fluids. Hence, is it relevant to
485 describe the current on-land hyper-alkaline springs as analogues of the MAR Lost City
486 hydrothermal system?

487

488 **Acknowledgements**

489 The authors would like to thank the Ministry of Water Resources of Oman for giving us
490 access to their data base on Oman springs. Financial support was provided by the CNRS-
491 INSU CESSUR Program. The authors would also like to thank the anonymous reviewers for
492 helpful comments and suggestions that no doubt improved this manuscript.

493

494 **References**

495 Abrajano, T.A., Sturchio, N.C., Bohlke, J.K., Lyon, G.L., Poreda, R.J., Stevens, C.M., 1988.
496 Methane-hydrogen gas seeps, Zambales Ophiolite, Philippines: Deep or shallow origin?,
497 Chem. Geol., 71 (1-3): 211–222.

498 Ague, J.J., 2000. Release of CO₂ from carbonate rocks during regional metamorphism of
499 lithologically heterogeneous crust, Geology 28 (12): 1123-1126.

500 Andreani, M., Munoz, M., Marcaillou, C., Delacour, A., 2013. μ XANES study of iron

501 speciation in serpentine during oceanic serpentinization. *Lithos* 178, 20–83.

502 Bach, W., Banerjee, N.R., Dick, H.J., Baker, E.T., 2002. Discovery of ancient and active
503 hydrothermal systems along the ultra-slow spreading Southwest Indian Ridge 10°-16°E.
504 *Geochem. Geophys. Geosyst.*, 3.

505 Barrett, T., Spooner, E., 1977. Ophiolitic breccias associated with allochthonous oceanic
506 crustal rocks in the East Ligurian Apennines, Italy — a comparison with observations from
507 rifted oceanic ridges. *Earth Planet. Sci. Lett.*, 35 (1): 79–91.

508 Benoit, M., Polvé, M., Ceuleneer, G., 1996. Trace element and isotopic characterization of
509 mafic cumulates in a fossil mantle diapir (Oman ophiolite). *Chem. Geol.*, 134 (1-3): 199–214.

510 Berndt, M.E., Allen, D.E., Seyfried, W.E., 1996. Reduction of CO₂ during serpentinization of
511 olivine at 300°C, *Geology* 24 (4): 351–354.

512 Bill, M., O’Dogherty, L., Guex, J., Baumgartner, P.O., Masson, H., 2001. Radiolarite ages in
513 Alpine-Mediterranean ophiolites: Constraints on the oceanic spreading and the Tethys-
514 Atlantic connection. *Geol. Soc. Am. Bull.* 113 (1): 129–143.

515 Blank, J.G., Green, S.J., Blake, D., Valley, J.W., Kita, N.T., Treiman, A., Dobson, P.F., 2009.
516 An alkaline spring system within the Del Puerto Ophiolite (California, USA): A Mars analog
517 site. *Planet. Space Sci.* 57 (5-6): 533–540.

518 Boschetti, T., Etiope, G., Toscani, L., 2013. Abiotic Methane in the Hyperalkaline Springs of
519 Genova, Italy. *Procedia Earth Planet. Sci.* 7: 248–251.

520 Boudier, F., Bouchez, J.L., Nicolas, A., Cannat, M., Ceuleneer, G., Misseri, M., Montigny, R.,
521 1985. Kinematics of oceanic thrusting in the Oman ophiolite: model of plate convergence.
522 *Earth Planet. Sci. Lett.* 75 (2-3): 215–222.

523 Boulart, C., Chavagnac, V., Delacour, A., Monnin, C., Ceuleneer, G., Hoareau, G., 2012.
524 New insights into gas compositions from hyperalkaline springs in Oman, Italy and New
525 Caledonia. Presented at the Serpentine Days 2012, Porquerolles, France.

526 Bradley, A.S., Summons, R.E., 2010. Multiple origins of methane at the Lost City
527 Hydrothermal Field. *Earth Planet. Sci. Lett.* 297 (1-2): 34–41.

528 Brouwer, F., Vissers, R.L.M., Lamb, W.M., 2002. Metamorphic History of Eclogitic
529 Metagabbro Blocks, From a Tectonic Mélange in the Voltri Massif, Ligurian Alps, Italy.
530 *Ofioliti* 1 (27): 1–16.

531 Bruni, J., Canepa, M., Chiadini, G., Cioni, R., Cipolli, F., Longinelli, A., Marini, L., Ottonello,
532 G., Vetuschi Zuccolini, M., 2002. Irreversible water-rock mass transfer accompanying the
533 generation of the neutral, Mg-HCO₃ and high-pH, Ca-OH spring waters of the Genova
534 province, Italy. *Applied Geochemistry* 17, 455–474.

535 Burns, S.J., Fleitmann, D., Matter, A., Neff, U., Mangini, A., 2001. Speleothem evidence
536 from Oman for continental pluvial events during interglacial periods. *Geology* 29 (7): 623–
537 626.

538 Busigny, V., Cartigny, P., Philippot, P., Ader, M., Javoy, M., 2003. Massive recycling of
539 nitrogen and other fluid-mobile elements (K, Rb, Cs, H) in a cold slab environment: evidence
540 from HP to UHP oceanic metasediments of the Schistes Lustrés nappe (western Alps, Europe).
541 *Earth Planet. Sci. Lett.* 215 (1-2): 27–42.

542 Cannat, M., Fontaine, F., Escartín, J., 2010. Serpentinization and associated hydrogen and
543 methane fluxes at slow spreading ridges, in: Rona, P.A., Devey, C.W., Dymant, J., Murton,
544 B.J. (Eds.), *Geophysical Monograph Series*. American Geophysical Union, Washington, D. C.,
545 pp. 241–264.

546 Capponi, G., Gosso, G., Scambelluri, M., Siletto, G.B., Tallone, S., 1994. Carta geologico-
547 strutturale del settore centro-meridionale del Gruppo di Voltri (Alpi liguri) e note illustrative.
548 *Boll. Soc. Geol. It.* 133: 383–394.

549 Ceuleneer, G., Monnereau, M., Amri, I., 1996. Thermal structure of a fossil mantle diapir
550 inferred from the distribution of mafic cumulates. *Nature* 379 (6561): 149–153.

551 Charlou, J.L., Donval, J.P., Fouquet, Y., Jean-Baptiste, P., Holm, N., 2002. Geochemistry of
552 high H₂ and CH₄ vent fluids issuing from ultramafic rocks at the Rainbow hydrothermal field
553 (36°14'N, MAR). *Chem. Geol.* 191 (4): 345–359.

554 Charlou, J.L., Donval, J.P., Konn, C., Ondréas, H., Fouquet, Y., Jean-Baptiste, P., Fourré, E.,
555 2010. High production and fluxes of H₂ and CH₄ and evidence of abiotic hydrocarbon
556 synthesis by serpentinization in ultramafic-hosted hydrothermal systems on the Mid-Atlantic
557 Ridge, in: Rona, P.A., Devey, C.W., Dymont, J., Murton, B.J. (Eds.), *Geophysical*
558 *Monograph Series*. American Geophysical Union, Washington, D. C., pp. 265–296.

559 Chavagnac, V., Ceuleneer, G., Monnin, C., Lansac, B., Hoareau, G., Boulart, C., 2013a.
560 Mineralogical assemblages forming at hyperalkaline warm springs hosted on ultramafic rocks:
561 A case study of Oman and Ligurian ophiolites: Mineral Precipitate at Alkaline Springs.
562 *Geochemistry, Geophysics, Geosystems* 14, 2474–2495.

563 Chavagnac, V., Monnin, C., Ceuleneer, G., Boulart, C., Hoareau, G., 2013b. Characterization
564 of hyperalkaline fluids produced by low-temperature serpentinization of mantle peridotites in
565 the Oman and Ligurian ophiolites: Hyperalkaline Waters in Oman and Liguria. *Geochemistry,*
566 *Geophysics, Geosystems* 14, 2496–2522.

567 Cipolli, F., Gambardella, B., Marini, L., Ottonello, G., Vetuschì Zuccolini, M., 2004.
568 Geochemistry of high-pH waters from serpentinites of the Gruppo di Voltri (Genova, Italy)
569 and reaction path modeling of CO₂ sequestration in serpentinite aquifers. *Appl. Geochem.* 19:
570 787–802.

571 Clark, I.D., Fontes, J.C., 1990. Palaeoclimatic reconstruction in northern Oman based on
572 carbonates from hyperalkaline groundwaters. *Quaternary Res.* 33: 320–336.

573 Connelly, D.P., Copley, J.T., Murton, B.J., Stansfield, K., Tyler, P.A., German, C.R., Van
574 Dover, C.L., Amon, D., Furlong, M., Grindlay, N., Hayman, N., Hühnerbach, V., Judge, M.,
575 Le Bas, T., McPhail, S., Meier, A., Nakamura, K., Nye, V., Pebody, M., Pedersen, R.B.,

576 Plouviez, S., Sands, C., Searle, R.C., Stevenson, P., Taws, S., Wilcox, S., 2012. Hydrothermal
577 vent fields and chemosynthetic biota on the world's deepest seafloor spreading centre. *Nature*
578 *Comm.* 3: 620.

579 Dal Piaz, G.V., Di Battistini, G., Gosso, G., Venturelli, G., 1980. Rodingitic gabbro dykes and
580 rodingitic reaction zones in the upper Valtournanche–Breuil area, Piemonte ophiolite nappe,
581 Italian Western Alps. *Archive Scientifique de Genève* 33: 161–179.

582 De Boer, J.Z., Chanton, J., Zeitlhöfler, M., 2007. Homer's chimaera (SW of Antalya/turkey);
583 burning abiogenic methane gases; are they generated by a serpentinization process related to
584 alkalic magmatism? *Ges. Geowiss.* 158 (4): 997–1003.

585 Des Marais, D.J., Donchin, J.H., Nehring, N.L., Truesdell, A.H., 1981. Molecular carbon
586 isotopic evidence for the origin of geothermal hydrocarbons. *Nature* 292 (5826): 826–828.

587 Dewandel, B., Lachassagne, P., Boudier, F., Al-Hattali, S., Ladouche, B., Pinault, J.-L., Al-
588 Suleimani, Z., 2005. A conceptual hydrogeological model of ophiolite hard-rock aquifers in
589 Oman based on a multiscale and a multidisciplinary approach. *Hydrogeol. J.* 13 (5-6): 708–
590 726.

591 Etiope, G., Schoell, M., Hosgörmez, H., 2011. Abiotic methane flux from the Chimaera seep
592 and Tekirova ophiolites (Turkey): Understanding gas exhalation from low temperature
593 serpentinization and implications for Mars. *Earth Planet. Sci. Lett.* 310 (1-2): 96–104.

594 Etiope, G., Tsikouras, B., Kordella, S., Ifandi, E., Christodoulou, D., Papatheodorou, G., 2013.
595 Methane flux and origin in the Othrys ophiolite hyperalkaline springs, Greece. *Chem. Geol.*
596 347: 161–174.

597 Etiope, G., Vance, S., Christensen, L.E., Marques, J.M., Ribeiro da Costa, I., 2013. Methane
598 in serpentinized ultramafic rocks in mainland Portugal. *Mar. Petrol. Geol.* 45: 12–16.

599 Evans, B.W., 2008. Control of the Products of Serpentinization by the Fe²⁺Mg-1 Exchange
600 Potential of Olivine and Orthopyroxene. *J. Petrol.* 49 (10): 1873–1887.

601 Ferrando, S., Frezzotti, M.L., Orione, P., Conte, R.C., Compagnoni, R., 2010. Late-Alpine
602 rodingitization in the Bellecombe meta-ophiolites (Aosta Valley, Italian Western Alps):
603 evidence from mineral assemblages and serpentinization-derived H₂-bearing brine. *Int. Geol.*
604 *Rev.* 52: 1220–1243.

605 Flory, P.G., 1936. Molecular size distribution in linear condensation polymers. *J. Am. Chem.*
606 *Soc.* 58: 1877–1885.

607 Fouquet, Y., Cherkashev, G., Charlou, J.-L., Ondreas, H., Birot, D., Cannat, M., Bortnikov,
608 M., Silantyev, S., Sudarikov, S., Cambon-Bonnavita, M.A., Desbruyeres, D., Fabri, M.-C.,
609 Querellou, J., Hourdez, S., Gebruk, A., Sokolova, T., Hoise, E., Mercier, E., Konn, C.,
610 Donval, J.P., Etoubleau, J., Normand, A., Stephan, M., Briand, P., Crozon, J., Fernagu, P.,
611 Buffier, E., 2008. Serpentine cruise—ultramafic hosted hydrothermal deposits on the Mid-
612 Atlantic Ridge: first submersible studies on Ashadze 1 and 2, Logatchev 2 and Krasnov vent
613 fields. *InterRidge News*, 17: 15–19.

614 Fournier, M., Lepvrier, C., Razin, P., Jolivet, L., 2006. Late Cretaceous to Paleogene post-
615 obduction extension and subsequent Neogen compression in the Oman Mountains. *GeoArabia*
616 11 (4): 17–40.

617 Glennie, K.W., Boeuf, M.G.A., Hughescl, M.W., Moodystu, M., Pilaar, W.F.H., Reinhard,
618 B.M., 1973. Late Cretaceous Nappes in Oman Mountains and their Geologic Evolution. *Am.*
619 *Assoc. Petr. Geol. Mem* 57 (1): 5–27.

620 Goodenough, K.M., Styles, M.T., Schofield, D., Thomas, R.J., Crowley, Q.C., Lilly, R.M.,
621 McKervey, J., Stephenson, D., Carney, J.N., 2010. Architecture of the Oman–UAE ophiolite:
622 evidence for a multi-phase magmatic history. *Arab. J. Geosci.* 3 (4): 439–458.

623 Green, E.J., 1958. A redetermination of the solubility of oxygen in seawater and some
624 thermodynamic implications of the solubility relations. University of California, Santa
625 Barbara. 138p.

626 Hamme, R.C., Emerson, S.R., 2004. The solubility of neon, nitrogen and argon in distilled
627 water and seawater. *Deep Sea Res. I* 51 (11): 1517–1528.

628 Hellevang, H., Huang, S., Thorseth, I.H., 2011. The Potential for Low-Temperature Abiotic
629 Hydrogen Generation and a Hydrogen-Driven Deep Biosphere. *Astrobiology* 11: 711–724.

630 Holm, N.G., Charlou, J.L., 2001. Initial indications of abiotic formation of hydrocarbons in
631 the Rainbow ultramafic hydrothermal system, Mid-Atlantic Ridge. *Earth Planet. Sci. Lett.* 191:
632 1 – 8.

633 Hoogerduijn Strating, E.H., 1991. The evolution of the Piemonte- Ligurian ocean. A
634 structural study of ophiolite complexes in Liguria (NW Italy). University of Utrecht, Utrecht.
635 127p.

636 Horita, J., Berndt, M.E., 1999. Abiogenic methane formation and isotopic fractionation under
637 hydrothermal conditions. *Science* 285: 1055 – 1057.

638 Hosgormez, H., 2007. Origin of the natural gas seep of Ciirali (Chimera), Turkey: Site of the
639 first Olympic fire. *J. Asian Earth Sci.* 30 (1): 131–141.

640 Ingmanson, D.E., Dowler, M.J., 1977. Ingmanson, D.E., Dowler, M.J., 1977. Chemical
641 evolution and the evolution of Earth's crust. *Origins of life*, 8: 221-224.

642 Katayama, I., Kurosaki, I., Hirauchi, K.-I., 2010. Low silica activity for hydrogen generation
643 during serpentinization: An example of natural serpentinites in the Mineoka ophiolite
644 complex, central Japan. *Earth Planet. Sci. Lett.* 298 (1-2), 199–204.

645 Kelley, D.S., Karson, J.A., Fruh-Green, G.L., Yoerger, D.R., Shank, T.M., Butterfield, D.A.,
646 Hayes, J.M., Schrenk, M.O., Olson, E.J., Proskurowski, G., Jakuba, M., Bradley, A., Larson,
647 B., Ludwig, K., Glickson, D., Buckman, K., Roe, K., Elend, M.J., Delacour, A., Bernasconi,
648 S.M., Lilley, M.D., Baross, J.A., Summons, R.E., Sylva, S.P., 2005. A Serpentinite-Hosted
649 Ecosystem: The Lost City Hydrothermal Field. *Science* 307, 1428–1434.

650 Klein, F., Bach, W., Jons, N., McCollom, T., Moskowitz, B., Berquo, T., 2009. Iron

651 partitioning and hydrogen generation during serpentinization of abyssal peridotites from 15°N
652 on the Mid-Atlantic Ridge. *Geochimica et Cosmochimica Acta* 73, 6868–6893.

653 Kolb, B., Ettore, L.S., 1997. *Static Headspace - Gas Chromatography: Theory and Practice*.
654 Wiley, New York. 376p.

655 Konn, C., Charlou, J.L., Donval, J.P., Holm, N.G., Dehairs, F., Bouillon, S., 2009a.
656 Hydrocarbons and oxidized organic compounds in hydrothermal fluids from Rainbow and
657 Lost City ultramafic-hosted vents. *Chem. Geol.* 258 (3-4): 299–314.

658 Konn, C., Holm, N., Donval, J.P., Charlou, J.-L., 2009b. Organic compounds in hydrothermal
659 fluids from ultramafic-hosted vents of the Mid Atlantic Ridge: an update on composition and
660 origin. *Geochim. Cosmochim. Acta* 73 (13 Suppl.): A679.

661 Kwarteng, A.Y., Dorvlo, A.S., Vijaya Kumar, G.T., 2009. Analysis of a 27-year rainfall data
662 (1977-2003) in the Sultanate of Oman. *Int. J. Climatol.* 29 (4): 605–617.

663 Lanphere, M.A., 1981. K-Ar ages of metamorphic rocks at the base of the Samail Ophiolite,
664 Oman. *J. Geophys. Res.* 86 (B4): 2777.

665 Launay, J., Fontes, J.C., 1985. Les sources thermales de Prony (Nouvelle Calédonie) et leurs
666 précipités chimiques. Exemple de formation de brucite primaire. *Géologie de la France* 1: 83–
667 100.

668 Lein, A.Y., Grichuk, D.V., Gurvich, E.G., Bogdanov, Y.A., 2000. A new type of hydrogen-
669 and methane-rich hydrothermal solutions in the Rift zone of the Mid-Atlantic Ridge. *Dokl.*
670 *Earth Sci.* 375A (9): 1304–1391.

671 Lyon, G.L., Giggenbach, W.F., Lupton, J.E., 1990. Composition and origin of the hydrogen-
672 rich gas seep, Fiordland, New Zealand. *EOS Trans.* V51D-10: 1717.

673 Malatesta, C., Crispini, L., Federico, L., Capponi, G., Scambelluri, M., 2011. The exhumation
674 of high pressure ophiolites (Voltri Massif, Western Alps): Insights from structural and
675 petrologic data on metagabbro bodies. *Tectonophysics.* 568-569: 102–103.

676 Marques, J.M., Carreira, P.M., Carvalho, M.R., Matias, M.J., Goff, F.E., Basto, M.J., Graça,
677 R.C., Aires-Barros, L., Rocha, L., 2008. Origins of high pH mineral waters from ultramafic
678 rocks, Central Portugal. *Appl. Geochem.* 23 (12): 3278–3289.

679 McCollom, T.M., Bach, W., 2009. Thermodynamic constraints on hydrogen generation
680 during serpentinization of ultramafic rocks. *Geochim. Cosmochim. Acta* 73 (3): 856–875.

681 McCollom, T.M., Seewald, J.S., 2001. A reassessment of the potential for reduction of
682 dissolved CO₂ to hydrocarbons during serpentinization of olivine. *Geochim. Cosmochim.*
683 *Acta* 65 (21): 3769–3778.

684 McCollom, T.M., Seewald, J.S., 2007. Abiotic Synthesis of Organic Compounds in Deep-Sea
685 Hydrothermal Environments. *Chem. Rev.* 107 (2): 382–401.

686 Mevel, C., 2003. Serpentinization of abyssal peridotites at mid-ocean ridges. *Comptes Rendus*
687 *Geosciences* 335, 825–852.

688 Montigny, R., Le Mer, O., Thuizat, R., Whitechurch, H., 1988. K-Ar and Ar study of
689 metamorphic rocks associated with the Oman ophiolite: Tectonic implications.
690 *Tectonophysics* 151 (1-4): 345–362.

691 Neal, C., Shand, P., 2002. Spring and surface water quality of the Cyprus ophiolites. *Hydrol.*
692 *Earth Syst. Sci.* 6 (5): 797–817.

693 Neal, C., Stanger, G., 1983. Hydrogen generation from mantle source rocks in Oman. *Earth*
694 *Planet. Sci. Lett.* 66: 315–320.

695 Neal, C., Stanger, G., 1984. Calcium and Magnesium Hydroxide Precipitation from Alkaline
696 Groundwaters in Oman, and Their Significance to the Process of Serpentinization.
697 *Mineralogical Magazine* 48 (347): 237–241.

698 Neubeck, A., Duc, N., Bastviken, D., Crill, P., Holm, N.G., 2011. Formation of H₂ and CH₄
699 by weathering of olivine at temperatures between 30 and 70°C. *Geochem. Trans.* 12: 6.

700 O’Hanley, D.S., Dyar, M.D., 1993. The composition of lizardite 1T and the formation of

701 magnetite in serpentinites. *American Mineralogist* 78, 844–844.

702 Oze, C., Sharma, M., 2005. Have olivine, will gas: Serpentinization and the abiogenic
703 production of methane on Mars. *Geophys. Res. Lett.* 32 (10).

704 Pearce, J.A., Alabaster, T., Shelton, A.W., Searle, M.P., 1981. The Oman Ophiolite as a
705 Cretaceous Arc-Basin Complex: Evidence and Implications. *Phil. Trans. R. Soc. A* 300
706 (1454): 299–317.

707 Peretti, A., Dubessy, J., Mullis, J., Frost, B.R., Trommsdorff, V., 1992. Highly reducing
708 conditions during Alpine metamorphism of the Malenco peridotite (Sondrio, Northern Italy)
709 indicated by mineral paragenesis and H₂ in fluid inclusions. *Contrib. Mineral. Petr.* 112: 329–
710 340.

711 Pfeifer, H.R., 1977. A model for fluids in metamorphosed ultramafic rocks. I Observations at
712 surface and subsurface conditions (high pH waters). *Schweiz. Mineral. Petrogr. Mitt.* 57:
713 361–396.

714 Philippot, P., Busigny, V., Scambelluri, M., Cartigny, P., 2007. Oxygen and nitrogen isotopes
715 as tracers of fluid activities in serpentinites and metasediments during subduction. *Mineral.*
716 *Petrol.* 91 (1-2): 11–24.

717 Power, I.M., Wilson, S.A., Thom, J.M., Dipple, G.M., Southam, G., 2007. Biologically
718 induced mineralization of dypingite by cyanobacteria from an alkaline wetland near Atlin,
719 British Columbia, Canada. *Geochem. Trans.* 8

720 Proskurowski, G., 2010. Abiogenic Hydrocarbon Production at the Geosphere-Biosphere
721 Interface via Serpentinization Reactions, in: Timmis, K.N. (Ed.), *Handbook of Hydrocarbon*
722 *and Lipid Microbiology*. Springer Berlin Heidelberg, Berlin, Heidelberg, pp. 215–231.

723 Proskurowski, G., Lilley, M.D., Seewald, J.S., Fruh-Green, G.L., Olson, E.J., Lupton, J.E.,
724 Sylva, S.P., Kelley, D.S., 2008. Abiogenic Hydrocarbon Production at Lost City
725 Hydrothermal Field. *Science* 319 (5863): 604–607.

726 Python, M., Ceuleneer, G., 2003. Nature and distribution of dykes and related melt migration
727 structures in the mantle section of the Oman ophiolite. *Geochem. Geophys. Geosyst.* 4 (7).

728 Python, M., Ceuleneer, G., Arai, S., 2008. Chromian spinels in mafic–ultramafic mantle
729 dykes: Evidence for a two-stage melt production during the evolution of the Oman ophiolite.
730 *Lithos* 106 (1-2): 137–154.

731 Python, M., Ceuleneer, G., Ishida, Y., Barrat, J.-A., Arai, S., 2007. Oman diopsidites: a new
732 lithology diagnostic of very high temperature hydrothermal circulation in mantle peridotite
733 below oceanic spreading centres. *Earth Planet. Sci. Lett.* 255 (3-4): 289–305.

734 Rioux, M., Bowring, S., Kelemen, P., Gordon, S., Miller, R., Dudás, F., 2013. Tectonic
735 development of the Samail ophiolite: High precision U-Pb zircon geochronology and Sm-Nd
736 isotopic constraints on crustal growth and emplacement. *J. Geophys. Res. Solid Earth.* 118.

737 Sader, J.A., Leybourne, M.I., McClenaghan, M.B., Hamilton, S.M., 2007. Low-temperature
738 serpentinization processes and kimberlite groundwater signatures in the Kirkland Lake and
739 Lake Timiskiming kimberlite fields, Ontario, Canada: implications for diamond exploration.
740 *Geochem.-Explor. Env. A* 7 (1): 3–21.

741 Sano, Y., Urabe, A., Wakita, H., Wushiki, H., 1993. Origin of hydrogen-nitrogen gas seeps,
742 Oman. *Appl. Geochem.* 8: 1–8.

743 Scambelluri, M., Philippot, P., 2004. Volatile and mobile element recycling during subduction
744 of the oceanic lithosphere. Insights from metasediments and serpentinites of the Alps. *Period.*
745 *Mineral.* 73 (Special Issue 2): 221–233.

746 Schandl, E.S., O’Hanley, D.S., Wicks, F.J., 1989. Rodingites in serpentinised ultramafic rocks
747 of the Abitibi greenstone belt, Ontario. *Can. Mineral.* 27: 579–591.

748 Schmidt, K., Koschinsky, A., Garbe-Schonberg, D., de Carvalho, L., Seifert, R., 2008.
749 Geochemistry of hydrothermal fluids from the ultramafic-hosted Logatchev hydrothermal
750 field, 15°N on the Mid-Atlantic Ridge: Temporal and spatial investigation. *Mar. Chem.* 108:

751 18–31.

752 Schwarzenbach, E.M., 2011. Serpentinization, fluids and life: Comparing carbon and sulfur
753 cycles in modern and ancient environments. ETH Zurich. 240p.

754 Schwarzenbach, E.M., Lang, S.Q., Früh-Green, G.L., Lilley, M.D., Bernasconi, S.M., Méhay,
755 S., 2013. Sources and cycling of carbon in continental, serpentinite-hosted alkaline springs in
756 the Voltri Massif, Italy. *Lithos* 177 : 226–244.

757 Seewald, J.S., Zolotov, M.Y., McCollom, T.M., 2006. Experimental investigation of single
758 carbon compounds under hydrothermal conditions. *Geochim. Cosmochim. Acta* 70 (2): 446–
759 460.

760 Seyfried, W.E., Foustoukos, D.I., Fu, Q., 2007. Redox evolution and mass transfer during
761 serpentinization: An experimental and theoretical study at 200°C, 500 bar with implications
762 for ultramafic-hosted hydrothermal systems at Mid-Ocean Ridges. *Geochim. Cosmochim.*
763 *Acta* 71 (15): 3872–3886.

764 Sherwood Lollar, B., Lacrampe-Couloume, G., Slater, G.F., Ward, J., Moser, D.P., Gihring,
765 T.M., Lin, L.-H., Onstott, T.C., 2006. Unravelling abiogenic and biogenic sources of methane
766 in the Earth's deep subsurface. *Chem. Geol.* 226 (3-4): 328–339.

767 Sherwood-Lollar, B., Lacrampe-Couloume, G., Voglesonger, K., Onstott, T.C., Pratt, L.M.,
768 Slater, G.F., 2008. Isotopic signatures of CH₄ and higher hydrocarbon gases from
769 Precambrian Shield sites: A model for abiogenic polymerization of hydrocarbons. *Geochim.*
770 *Cosmochim. Acta* 72 (19): 4778–4795.

771 Shock, E.L., 1990. Geochemical constraints on the origin of organic compounds in
772 hydrothermal systems. *Origins Life Evol. B.* 20: 331–367.

773 Smith, R.J., Duerksen, J.D., 1975. Glycerol inhibition of purified and chromatin-associated
774 mouse liver hepatoma RNA polymerase II activity. *Biochem. Biophys. Res. Commun.* 67 (3):
775 916–923.

776 Taran, Y.A., Varley, N.R., Inguaggiato, S., Cienfuegos, E., 2010. Geochemistry of H₂- and
777 CH₄-enriched hydrothermal fluids of Socorro Island, Revillagigedo Archipelago, Mexico.
778 Evidence for serpentinization and abiogenic methane. *Geofluids* 10 (4): 542–555.
779 Tilton, G.R., Hopson, C.A., Wright, J.E., 1981. Uranium-lead isotopic ages of the Samail
780 Ophiolite, Oman, with applications to Tethyan ocean ridge tectonics. *J. Geophys. Res.* 86
781 (B4): 2763.
782 Tippit, P.R., Pessagno, E.A., Smewing, J.D., 1981. The biostratigraphy of sediments in the
783 volcanic unit of the Samail Ophiolite. *J. Geophys. Res.* 86 (B4): 2756.
784 Vignaroli, G., Rossetti, F., Rubatto, D., Theye, T., Lisker, F., Phillips, D., 2010. Pressure-
785 temperature-deformation-time (P-T-d-t) exhumation history of the Voltri Massif HP complex,
786 Ligurian Alps, Italy. *Tectonics* 29 (6): TC6009.

787

788 **Table and Figure Captions**

789

790 **Table 1:** Chemical composition, geological settings and precipitates of the Oman and Liguria
791 hyperalkaline springs. Sampling indicates the type of sample collected (G: gas/DG: dissolved
792 gas).

793 **Table 2:** Chemical compositions of the gases collected in Oman and Liguria hyperalkaline
794 springs. n.d.: not detected.

795 **Table 3:** Concentration of the dissolved gases in the Oman and Liguria hyperalkaline waters.
796 Concentrations are given in $\mu\text{mol/l}$. n.d.: not detected.

797 **Figure 1:** Simplified geological map of the Oman ophiolite showing the locations of the
798 investigated springs. For a better comprehension of the surface lithology, the reader may refer
799 to Table 1 where details are given.

800 **Figure 2:** Simplified geological map of the Voltri Massif (Liguria, Italy) showing the

801 locations of the investigated springs. Stars indicate the two stations where active gas bubbling
802 was observed.

803 **Figure 3:** The variation of the K/Cl ratio of the alkaline waters versus the N₂/O₂ ratio of the
804 gases for the Liguria and Oman springs.

805 **Figure 4:** Mean H₂/CH₄ ratios for our samples (Oman 2011 and Liguria 2010) compared with
806 various ultramafic environments showing three distinct gas composition groups. Data used
807 here are from Abrajano et al, 1988 (Zambales); Charlou et al., 2002 (Rainbow);
808 Proskurowsky et al., 2008 (Lost City); Taran et al., 2010 (Socorro Island); Etiope et al, 2011
809 (Tekirova); Boulart et al., 2012 (Bay of Prony); Etiope et al, 2013 (Othrys); Schmidt et al.,
810 2008 (Logatchev); Etiope et al., 2013b (Portugal); Boschetti et al., 2013 (Liguria 2013). Error
811 bars indicate the standard deviation of the gas concentration distribution. Note that Rainbow
812 and Logatchev are considered as high-temperature vent sites (T>350°C) while Lost City is
813 ~90-100°C. The on-land venting sites are considered as low-temperature (T<40°C). In red,
814 sites developing in a mid-ocean ridge context and in blue in a subduction context.

815 **Figure 5:** The oxygen (O₂) versus hydrogen partial pressure of the Liguria and Oman gases

816 **Figure 6:** The dissolved SiO₂ concentration versus the CH₄(g) partial pressure for the Oman
817 and Liguria springs.

818 **Figure 7:** Logarithmic distribution of mole fraction as a function of carbon number for Sites
819 11, 13, 20 and 27 in Oman showing that the Oman hydrocarbon composition does not fit the
820 Schulz-Flory distribution. Dashed line represent a distribution typical of abiotic synthesis
821 (Sherwood Lollar et al., 2008). Mole fraction is calculated as $x_i = n_i/n_{tot}$ with n_i as the amount
822 of i constituent and n_{tot} the total amount of all constituents.

823 **Figure 8:** The CH₄(g) partial pressure versus that of ethane for the Oman and Liguria gases.

Figure 1

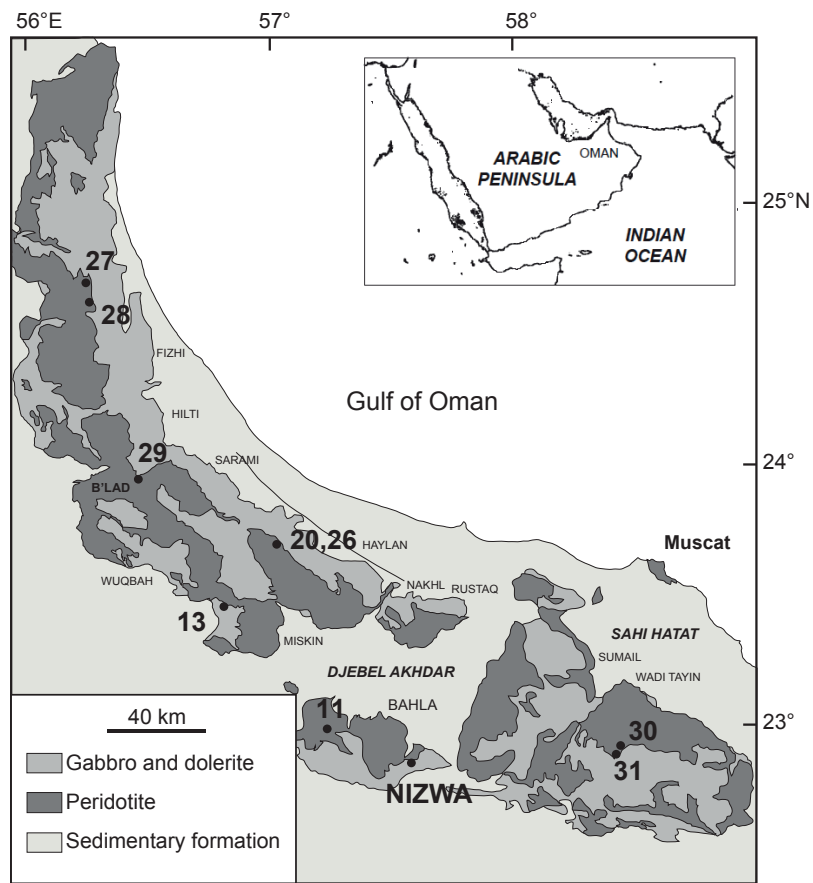


Figure 2

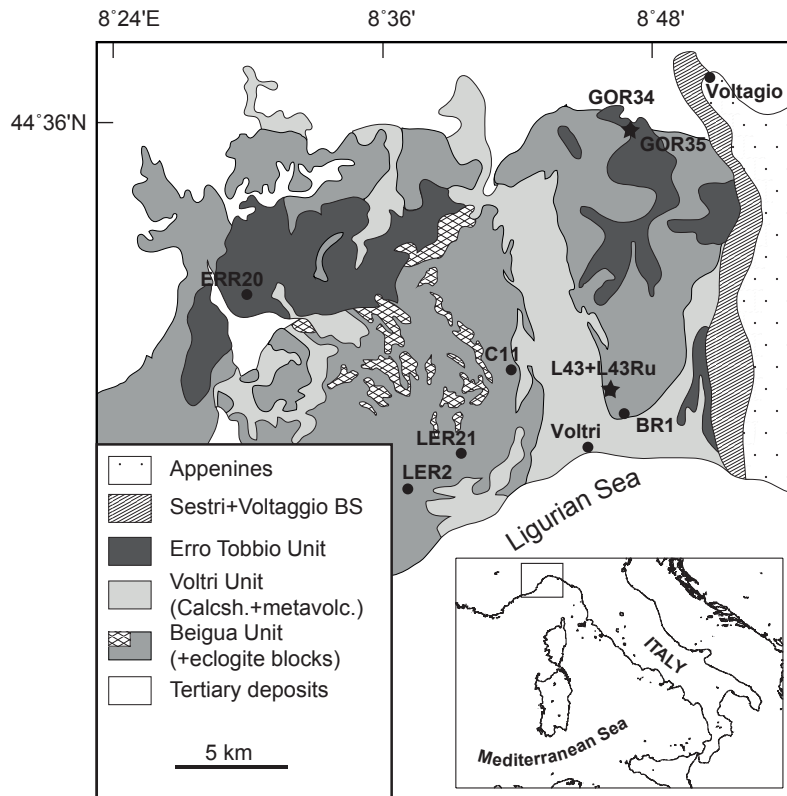


Figure 3

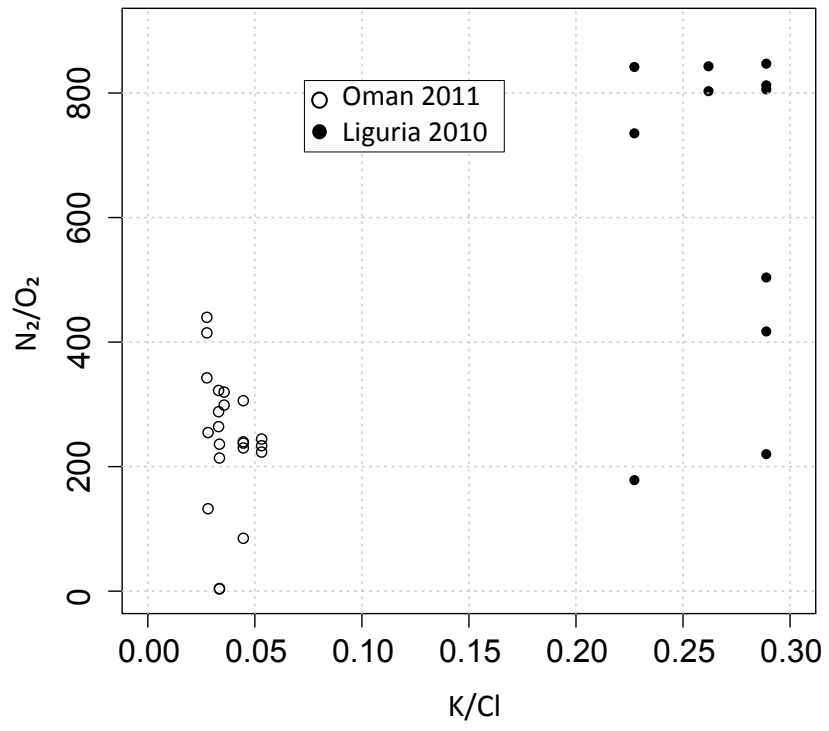


Figure 4

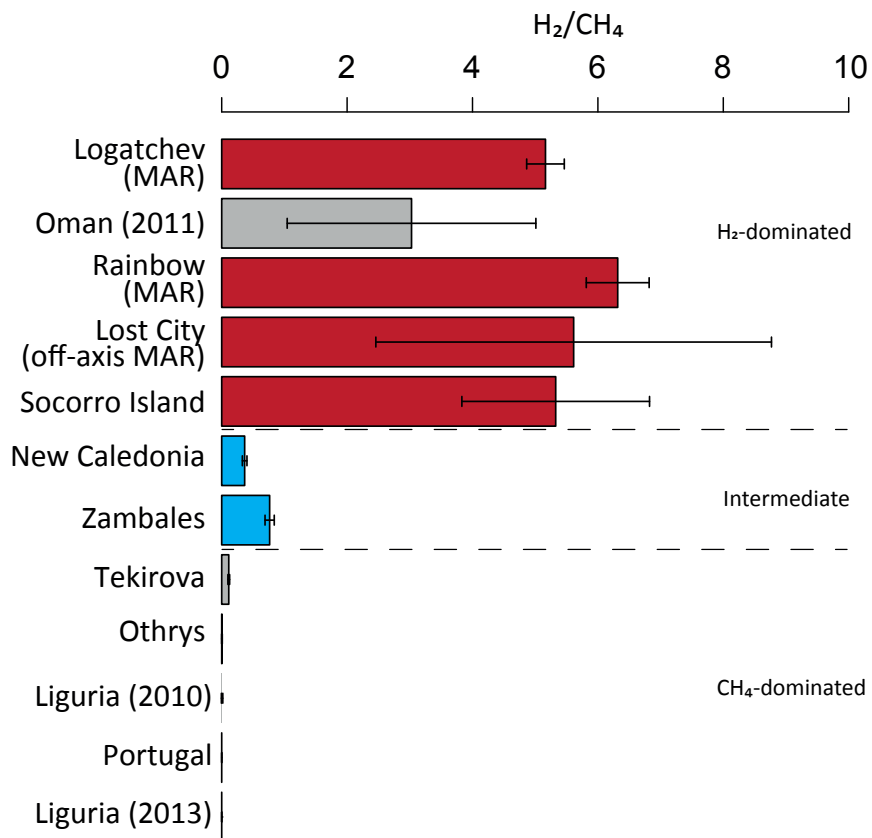


Figure 6

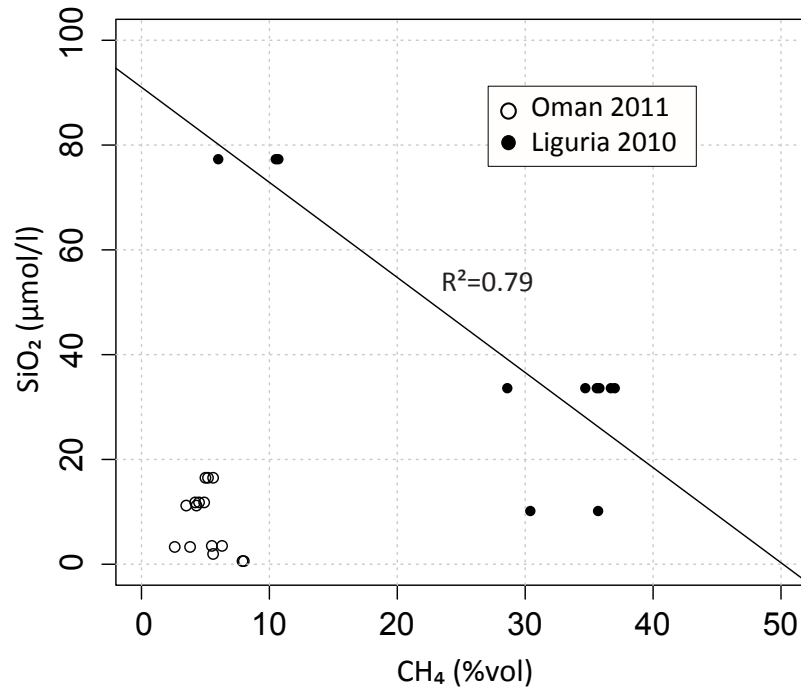


Figure 7

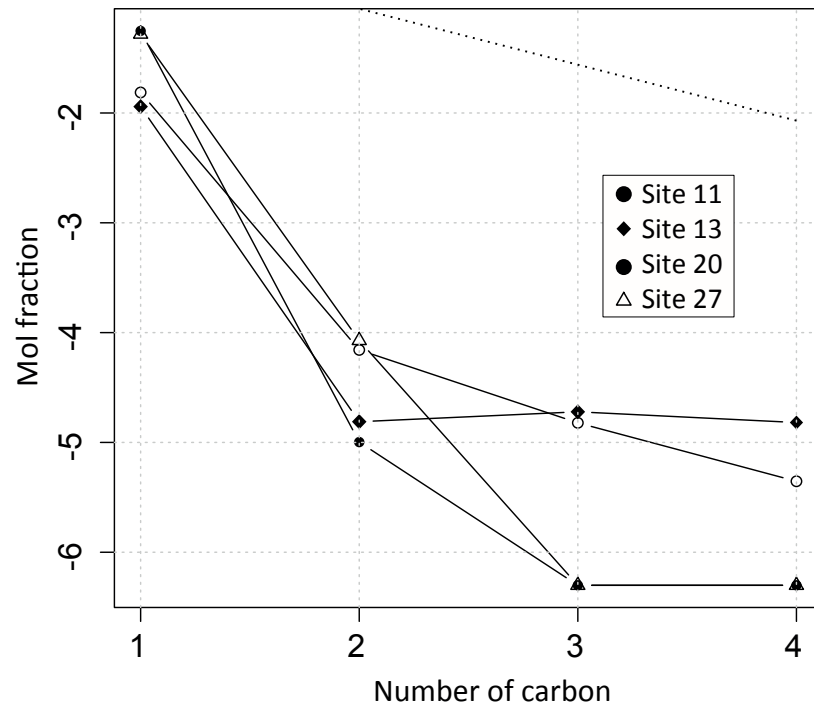


Figure 8

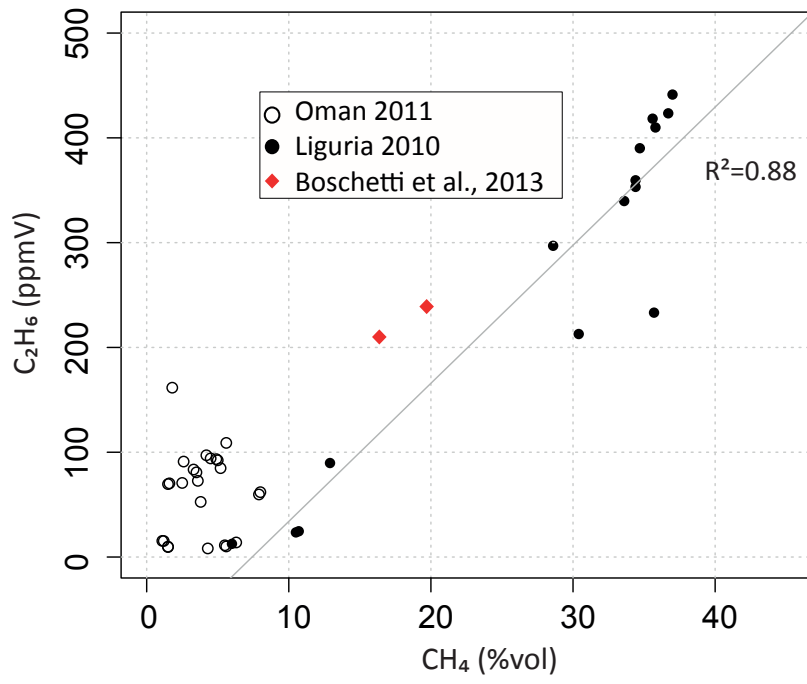


Table 1

Sites	Latitude N	Longitude E	T (°C)	pH	SiO ₂ (mmol/l)	Mg (mmol/l)	Ca (mmol/l)	K (mmol/l)	Na (mmol/l)	Cl (mmol/l)	Sampling	Geology	Precipitates
<i>Oman</i>													
Site 11	22.9880	57.2890	28.3	11.6	0.05	0.47	0.81	0.27	6.46	5.01	G/DG	Serpentinite	
Site 13	23.4033	56.8577	28.0	11.7	0.00	0.00	1.87	0.16	6.84	4.80	G/DG	peridotite/gabbro, MOHO	Aragonite, Brucite
Site 20	23.6232	57.1092	29.4	11.2	0.04	0.82	0.15	0.18	4.82	3.83	G/DG	Bedded gabbro above peridotite (100 m thick)	Aragonite, Brucite
Site 26	23.6187	57.1080	31.3	11.3	0.02	0.00	0.66	0.22	5.83	3.95	DG	Peridotite (100 m above the Moho)	Aragonite, Brucite
Site 27	24.7008	56.2692	31.2	11.1	0.12	1.40	0.51	0.08	3.02	2.12	G/DG	Wherlite/gabbro, within the crustal section	Aragonite
Site 28	24.5242	56.2845	30.7	10.1	0.08	1.13	0.61	0.09	3.17	3.17	G/DG	Bedded gabbro and ultramafic cumulates, within the crustal section	Aragonite, Mg-calcite, Brucite
Site 29	23.9572	56.4377	23.8	11.6	0.00	0.00	1.03	0.15	6.64	3.83	DG	Serpentinite with gabbro 100 m above	Aragonite (brucite)
Site 30	22.9037	58.4225	27.5	11.7	0.02	b.d.l.	1.96	0.14	6.65	2.81	DG	Peridotite	Aragonite, Brucite
Site 31	22.8907	58.3902	26.4	11.6	0.16	1.83	0.66	0.07	3.49	2.87	G/DG	Peridotite near MOHO	Aragonite (brucite)
<i>Liguria</i>													
ERR20	44.508793	8.499098	23.7	11.1	51.31	0.00	0.33	0.05	0.74	0.50	DG	Serpentinite + metagabbros	Calcite
C11	44.469	8.695346	14.0	11.5	3.62	0.23	0.07	0.04	0.57	0.60	DG	Serpentinite + metagabbros	Calcite
GOR34	44.596363	8.783641	23.7	11.6	10.17	0.01	0.85	0.11	0.85	0.42	G	serpentinised lherzolites	Calcite+Aragonite
GOR35	44.59655	8.786923	21.4	11.2	45.10	0.12	0.46	0.05	0.32	0.22	G/DG	serpentinised lherzolites	Calcite
L43	44.458	8.768944	22.6	11.7	33.77	n.a.	0.76	0.13	1.26	0.45	G/DG	Serpentinite + metagabbros	Calcite
L43Ru	44.458	8.768944	20.0	11.6	n.a.	n.a.	n.a.	n.a.	n.a.	n.a.	G	Serpentinite + metagabbros	Calcite
BR1	44.445473	8.778927	17.3	11.5	25.88	n.a.	0.75	0.08	1.05	0.50	DG	Serpentinite + metagabbros	Calcite
LER21	44.424297	8.6582717	17.5	11.3	4.97	n.a.	0.72	0.02	0.43	0.55	DG	Serpentinite + metagabbros	Calcite
LER2	44.40568	8.618569	17.3	9.5	17.84	0.01	0.56	0.10	0.45	0.56	DG	Serpentinite + metagabbros	Calcite

Table 2

Sites	CH ₄ (%vol)	H ₂ (%vol)	N ₂ (%)	O ₂ (ppmV)	CO (ppmV)	CO ₂ (ppmV)	C ₂ H ₆ (ppmV)	C ₃ H ₈ (ppmV)	C ₄ H ₁₀ (ppmV)	C ₅ H ₁₂ (ppmV)
<i>Oman 2011</i>										
Site 11	1.5	10.6	12.4	507.6	n.d.	n.d.	69.6	15.1	4.4	n.d.
Site 11	1.6	10.7	12.7	543.8	n.d.	n.d.	70.3	14.7	5.2	n.d.
Site 11	2.5	11.1	12.7	568.6	n.d.	n.d.	70.7	14.9	5.8	n.d.
Site 13	1.5	10.5	11.2	474.6	n.d.	n.d.	9.9	8.2	n.d.	n.d.
Site 13	1.5	11.3	12.2	570.7	n.d.	n.d.	9.5	7.8	5.7	8.2
Site 20	5.6	11.2	13.3	559.5	n.d.	n.d.	10.1	n.d.	n.d.	n.d.
Site 20	5.5	11.3	12.7	552.3	n.d.	n.d.	11.2	n.d.	n.d.	n.d.
Site 20	6.3	10.9	13.5	563.0	n.d.	n.d.	13.9	n.d.	n.d.	n.d.
Site 20	4.3	11.0	12.8	418.5	n.d.	n.d.	8.2	n.d.	n.d.	n.d.
Site 27	5.2	9.6	25.0	568.5	n.d.	n.d.	84.8	n.d.	n.d.	n.d.
Site 27	5.6	10.0	27.0	788.2	n.d.	n.d.	108.9	n.d.	n.d.	n.d.
Site 27	5.0	9.4	24.0	578.6	n.d.	n.d.	92.3	n.d.	n.d.	n.d.
Site 28B	3.3	10.4	18.0	970.9	n.d.	n.d.	83.5	n.d.	n.d.	n.d.
Site 28B	3.6	10.4	15.5	497.6	n.d.	n.d.	72.7	n.d.	n.d.	n.d.
Site 28C	2.6	9.9	21.7	1639.1	n.d.	n.d.	91.1	n.d.	n.d.	n.d.
Site 28C	3.8	10.7	15.7	616.4	n.d.	n.d.	52.6	n.d.	n.d.	n.d.
Site 28D	4.2	11.0	15.5	480.9	n.d.	n.d.	97.1	n.d.	n.d.	n.d.
Site 28D	4.9	11.5	17.6	610.8	n.d.	n.d.	93.4	n.d.	n.d.	n.d.
Site 28D	4.5	12.1	17.8	673.7	n.d.	n.d.	94.1	n.d.	n.d.	n.d.
Site 31	7.9	10.7	15.7	491.0	n.d.	n.d.	59.7	n.d.	n.d.	n.d.
Site 31	8.0	10.7	15.9	532.1	n.d.	n.d.	61.9	n.d.	n.d.	n.d.
<i>Liguria 2010</i>										
GOR34	35.7	0.2	35.9	447.1	n.d.	n.d.	233.2	n.d.	n.d.	n.d.
GOR34	30.4	0.0	31.5	373.7	n.d.	106.7	212.8	n.d.	n.d.	n.d.
GOR35	10.5	0.0	33.8	459.7	n.d.	107.5	23.5	n.d.	n.d.	n.d.
GOR35	10.7	1.2	33.8	401.5	n.d.	106.7	24.6	n.d.	n.d.	n.d.
L43Ru	34.4	1.0	32.4	559.3	39.2	124.9	359.5	n.d.	n.d.	n.d.
L43Ru	34.4	0.0	32.0	480.3	n.d.	129.7	353.2	n.d.	n.d.	n.d.
L43Ru	33.6	0.0	31.0	386.0	n.d.	123.5	339.7	n.d.	n.d.	n.d.
L43	37.0	0.0	30.7	381.0	n.d.	n.d.	441.3	n.d.	n.d.	n.d.
L43	34.7	0.0	30.7	736.1	n.d.	106.2	390.1	n.d.	n.d.	n.d.
L43	35.6	0.1	31.3	621.4	n.d.	106.5	418.3	n.d.	n.d.	n.d.
L43	36.7	0.1	30.3	373.0	n.d.	n.d.	423.4	n.d.	n.d.	n.d.
L43	35.8	0.0	30.2	356.5	n.d.	n.d.	409.9	n.d.	n.d.	n.d.

Table 3

Sites	Samples	H ₂	CH ₄	N ₂	O ₂	CO	CO ₂	C ₂ H ₆
<i>Oman</i>								
<i>2011</i>								
Site 11	GD1	214.6	36.3	1281.4	13.4	n.d.	n.d.	0.24
Site 11	GD2	215.7	38.4	762.6	7.4	n.d.	n.d.	0.28
Site 13	GD1	333.2	25.4	848.8	7.9	n.d.	n.d.	n.d.
Site 13	GD2	340.8	28.0	725.1	8.7	n.d.	n.d.	n.d.
Site 20	GD2 GV	222.3	96.5	755.2	8.8	n.d.	n.d.	n.d.
Site 20	GD2 PV	341.7	147.6	725.7	7.2	n.d.	n.d.	n.d.
Site 20	GD2 Wadi	26.7	15.1	995.5	12.3	n.d.	n.d.	n.d.
Site 20	GD3 Wadi	65.1	15.5	848.5	10.7	n.d.	n.d.	n.d.
Site 26	GD2	168.6	7.4	846.3	6.7	n.d.	n.d.	n.d.
Site 27	GD1	132.1	84.7	823.6	7.4	n.d.	n.d.	n.d.
Site 27	GD5	184.9	15.4	892.2	11.0	n.d.	n.d.	n.d.
Site 27b	GD1	179.3	71.9	821.6	7.4	n.d.	n.d.	n.d.
Site 27b	GD2	59.4	39.5	2135.2	23.4	n.d.	n.d.	n.d.
Site 28C	GD2	274.2	64.6	1661.4	15.1	n.d.	n.d.	n.d.
Site 28D	GD2	115.7	25.3	872.7	10.4	n.d.	n.d.	n.d.
Site 28G	GD1	377.5	70.2	656.6	5.7	n.d.	n.d.	n.d.
Site 29	GD1	219.5	38.0	827.7	8.2	n.d.	n.d.	n.d.
Site 29	GD2	168.0	31.1	825.8	8.4	n.d.	n.d.	n.d.
Site 30	GD2	338.9	209.2	794.7	8.7	n.d.	n.d.	0.15
Site 30	GD1	227.2	206.0	839.0	9.2	n.d.	n.d.	0.14
Site 31	GD1	48.0	64.4	1382.3	14.9	n.d.	n.d.	n.d.
Site 31	GD1	225.0	68.2	976.2	12.3	n.d.	n.d.	n.d.
Site 31	GD1	98.5	21.1	850.3	10.5	n.d.	n.d.	n.d.
<i>Liguria 2010</i>								
ERR20	2GD	3.8	19.0	711.2	5.2	0.03	0.99	n.d.
ERR20	1GD	4.3	5.8	691.6	4.2	0.02	0.99	n.d.
C11	1GD	1.2	384.5	1066.5	9.7	n.d.	1.23	n.d.
C11	3GD	0.5	349.7	1184.6	11.7	n.d.	1.23	n.d.
C11	2GD	14.6	456.6	806.5	5.0	n.d.	1.18	n.d.
GOR35	1GD	5.8	88.1	1186.7	11.0	n.d.	1.09	n.d.
L43	1GD	2.1	649.4	600.6	3.3	n.d.	1.00	n.d.
BR1	1GD	3.0	279.9	1131.8	10.8	n.d.	1.18	n.d.
BR1	2GD	0.3	278.2	1113.4	10.5	n.d.	1.14	n.d.
BR1	3GD	5.8	285.8	951.4	8.3	n.d.	1.10	n.d.
LER21	1GD	0.0	57.0	1134.8	10.8	n.d.	1.21	n.d.
LER21	2GD	2.5	50.8	1155.6	11.0	n.d.	1.25	n.d.
LER21	3GD	4.1	54.2	1091.4	10.1	n.d.	1.11	n.d.
LER2	1GD	561.6	0.8	3784.9	31.6	n.d.	21.52	n.d.
LER2	3GD	66.7	0.0	2041.2	18.0	n.d.	22.19	n.d.